Adsorption and heterogeneous advanced oxidation of phenolic contaminants using Fe loaded mesoporous SBA-15 and H_2O_2

Pradeep Shukla, Shaobin Wang*, Hongqi Sun, Hua-Ming Ang, Moses Tadé

Department of Chemical Engineering and CRC for Contamination Assessment and Remediation of the Environment (CRC-CARE), Curtin University of Technology, GPO Box U1985, Perth, WA 6845, Australia

ARTICLE INFO

ABSTRACT

Mesoporous silica, SBA-15, supported Fe/SBA-15 catalysts were prepared by impregnation and tested for adsorption and heterogeneous advanced oxidation of 2,4-dichlorophenol (DCP) in aqueous solution using H_2O_2. Characterisation indicated that Fe impregnation did not change the porous structure of SBA-15. Fe/SBA-15 exhibits moderate DCP adsorption, however, Fe/SBA-15 is effective for DCP oxidation under H_2O_2. The catalytic activity depends on Fe loading, H_2O_2 concentration, DCP concentration and solution pH. Fe/SBA-15 can achieve 100% DCP conversion and 60% TOC removal at the conditions of 100 ppm DCP, 0.05 g 10%wt Fe/SBA-15, and 1000 ppm H_2O_2. This catalyst also shows stable performance with low Fe leaching.

1. Introduction

Currently, many industrial processes produce wastewater containing organic refractory compounds. These compounds can be removed by adsorption onto porous solids like activated carbon, clays and mesoporous solids, but this process only transfers the contaminants from liquid phase to solid phase. Advanced oxidation processes show advantages in complete decomposition and removal of these compounds [1].

It is well known that the oxidation process by the Fenton reagent (Fe^{2+}/H_2O_2) is the most widely used technique in treatment of organic pollutants in aqueous solution. However, this process is limited by acidic pH requirement (pH 2–4), high amount of sludge in the coagulation step, and loss of Fe ions in water. Heterogeneous Fenton oxidation provides an alternative to the homogeneous oxidation for the reaction occurred at high pH and recyclable use of Fe catalysts. In the past few years, attempts have been made to develop various Fe-based catalysts using oxides and supported oxides [2–8].

Since the discovery of ordered mesoporous silica materials in 1990s, synthesis and applications of mesoporous solids have received an intensive attention due to their highly ordered structure, larger pore size, and high surface area [9,10]. However, few investigations have been reported in using mesoporous materials for heterogeneous Fenton oxidation. Gokulakrishnan et al. [11] synthesised mesoporous Fe-MCM-41 molecular sieves (Si/Fe = 25, 50, 75 and 100) by a hydrothermal co-condensation method and evalu-

ated the behaviour in removal of citric acid from aqueous solution by the wet peroxidation. They found that more mineralisation of citric acid was achieved by heterogeneous catalysis with Fe-MCM-41 with the percentage removal of total organic carbon (TOC) of citric acid following the order Fe-MCM-41 (Si/Fe = 25) > Fe-MCM-41 (Si/Fe = 50) > Fe-MCM-41 (Si/Fe = 75) > Fe-MCM-41 (Si/Al = 100). Martinez et al. [12] investigated heterogeneous photo-Fenton degradation of phenolic aqueous solutions over iron-containing SBA-15 catalysts. Melero et al. [13] also reported a nanocomposite of crystalline Fe_2O_3 and CuO particles with mesostructured SBA-15 silica as an active catalyst for wet peroxide oxidation processes. They found that the presence of copper prevents the leaching of iron species and increases TOC degradation. Lim et al. [14] reported a highly active heterogeneous Fenton catalyst using iron oxide nanoparticles immobilised in alumina coated mesoporous silica. Recently, Botas et al. [15] prepared different iron-containing catalysts on mesostructured SBA-15 silica and non-ordered mesoporous silica for the oxidation of phenol aqueous solution in a catalytic fixed bed reactor in the presence of hydrogen peroxide.

In the most previous investigations, Fe was loaded on mesoporous solid by sol–gel co-condensation and phenol as a typical pollutant, few works were reported on impregnation and other organic compounds. In general, impregnation can achieve higher loading of Fe on mesoporous supports. In addition, other organic compounds may show different decomposition behaviours on heterogeneous Fenton catalysts. The current work discusses the loading of ferrous oxide on the mesoporous silica (SBA-15) and the application of this material for combined adsorption and oxidation of 2,4-dichlorophenol (DCP).

* Corresponding author. Tel.: +61 8 9266 3776; fax: +61 8 9266 2681.
E-mail address: shaobin.wang@curtin.edu.au (S. Wang).

2. Experimental

2.1. Preparation of SBA-15 and Fe/SBA-15

The synthesis of mesoporous silica SBA-15 was prepared following the procedure described by Zhao et al. [16] using a tri-block copolymer, poly(ethylene glycol)-block-poly(propylene glycol)-block-poly(ethylene glycol) EO_{20}-PO_{70}-EO_{20} as the template agent and tetra ethyl orthosilicate (TEOS) as a silica source, respectively. In a typical synthesis, 12 g of tri-block copolymer and 13.44 g of KCl were dissolved in 360 ml of 2 M HCl solution with stirring at 40 °C and then 22.96 g of TEOS was added into the solution with vigorous stirring for 8 min. The mixture was kept aging under static condition for 24 h at the same temperature. The resulted mixture was transferred to an autoclave and kept at 100 °C for 24 h. The SBA-15 silica product was then filtered, washed with distilled water and dried at 50 °C. The polymeric structure-directing agent (EO_{20}-PO_{70}-EO_{20}) was removed by calcination at 550 °C for 5 h in air.

$FeSO_4$ obtained from Sigma–Aldrich was used as the precursor of ferrous ion. During the preparation of Fe/SBA-15 catalysts, a fixed amount of the Fe precursor was dissolved in water to obtain 4 or 10 wt% Fe on the prepared SBA-15. The solution was firstly flushed with nitrogen to remove any dissolved oxygen. Predetermined amount of the prepared SBA-15 was then added to the solution and the solution was stirred under nitrogen atmosphere for 24 h for impregnation of Fe ions in SBA-15. The solution was then heated to remove the solvent and was further calcined at 500 °C for 6 h.

2.2. Characterisation of Fe/SBA-15 catalysts

The catalysts were characterised using several techniques to identify the structural and physicochemical properties. The crystalline form of the catalyst was identified by X-ray diffractometer (XRD) on a Bruker D8 advanced research XRD with Cu Kα radiation at a scanning rate of 2°/min. N_2 adsorption was used to obtain surface area on a NOVA 1200 adsorption analyser (Quantachrome). Fourier transform infrared (FT-IR) analysis was done to identify the functional groups associated with the catalyst. FT-IR spectra were collected on a Perkin Elmer, Spectrum 100 spectrophotometer with an attenuated total reflectance (ATR) technique. The spectrum was scanned from 400 to 4000 cm^{-1}. The morphology of SBA-15 and the catalyst was studied using SEM. Elemental composition was identified by EDX. Fe loading is analysed by digesting the catalyst in an acid solution to remove the metal and measuring the concentration of Fe ions using an ICP-MS (Agilent, 7700).

2.3. Adsorption of 2,4-dichlorophenol on Fe/SBA-15

The adsorption tests were carried out in 30 ml bottles, wherein a fixed amount of the adsorbent (approximately 0.02 g) was added to 2,4-dichlorophenol solutions with varying concentrations. The adsorbate concentration was ranged from 50 to 500 ppm. The solution was filled exactly till the top of the sample bottles and sealed properly to prevent any evaporation loss. Preliminary tests showed that adsorption equilibrium could be reached in 1 d. The bottles were kept in an incubator shaker, set at the temperature of 25 °C and a speed of 200 rpm for 3 d to make adsorption longer enough for adsorption equilibrium. One ml of sample was acquired from the sample bottles using a syringe filter, and analysed by a HPLC having a UV detector at the fixed wavelength of 270 nm for all the components. A blank sample without any adsorbent was also kept together with the experimental samples to monitor any change of concentration due to evaporation or precipitation; however, the analysis of the blank sample showed negligible loss of the adsorbate.
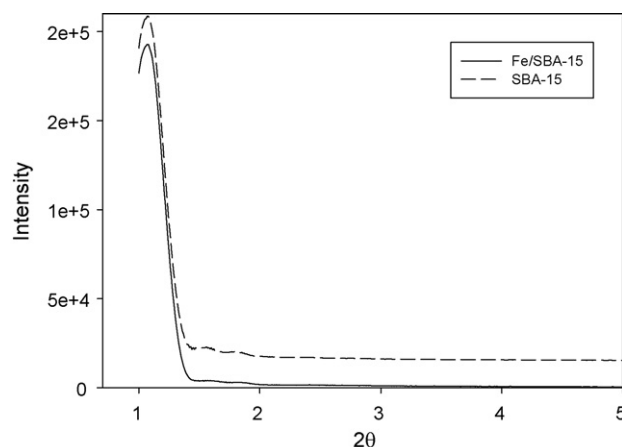

Fig. 1. XRD profiles of SBA-15 and Fe/SBA-15.

2.4. Kinetic study of 2,4-dichlorophenol oxidative destruction

A batch reactor with 1 L was employed. For each run, 500 ml of 2,4-dichlorophenol (DCP) solution at varying concentrations was added to the reactor and stirred at 200 rpm to homogenise the solution. A fixed amount of Fe/SBA-15 catalyst was added to the reactor, followed by the addition of hydrogen peroxide to start the oxidation. The reactor vessel was suspended in a water bath to maintain the reaction temperature at 25 °C. During the reaction, 1 ml sample was extracted at fixed intervals using a syringe filter and quenched with excess methanol to stop the reaction. The samples were analysed for DCP concentration using a Varian HPLC having a UV detector at 270 nm. The column used was C-18 and the mobile phase was 30% CH_3CN and 70% water with a flow rate of 1.5 ml/min. For TOC analysis, 1 ml sample was withdrawn at interval of a fixed time, quenched with excess sodium nitrite and then tested for the TOC on a Shimadzu TOC analyser (TOC-5000 CE).

3. Results and discussion

3.1. Characterisation of SBA-15 and Fe/SBA-15

XRD patterns of SBA-15 and Fe/SBA-15 are displayed in Fig. 1. It is clearly seen that SBA-15 shows three distinct peaks at (1 0 0), (1 1 0) and (2 0 0) reflections, typical of hexagonally mesostructured material. Fe/SBA-15 also shows the strong peak at (1 0 0), demonstrating the similar mesoporous structure as SBA-15.

Fig. 2 presents a SEM photo and EDX profile of Fe/SBA-15. The morphology obtained by SEM shows the uniform size particles with elongated hexagonal structure. The particle size varies in a range of 0.85–1.5 μm. The EDX spectrum of Fe loaded SBA-15 confirms the presence of Fe in the particles.

FT-IR spectra of SBA-15 and Fe/SBA-15 (Fig. 3) show major peaks at 1074 and 1214 cm^{-1} representing the IR absorption of Si–O–Si. The broad peak at 3409 cm^{-1} represents the O–H vibrations, which could be due to the presence of silanol group or OH group of adsorbed water molecule. The spectra of SBA-15 and Fe/SBA-15 were similar. This confirms that there was no significant change in the functional groups due to ion loading on SBA-15 support.

3.2. Adsorption of 2,4-dichlorophenol on Fe/SBA-15

Fig. 4 shows the adsorption isotherm of DCP on SBA-15 and Fe/SBA-15. As seen, SBA-15 exhibits higher DCP adsorption than Fe/SBA-15. DCP adsorption increases with increasing equilibrium concentration. At 500 ppm equilibrium concentration, the adsorp-
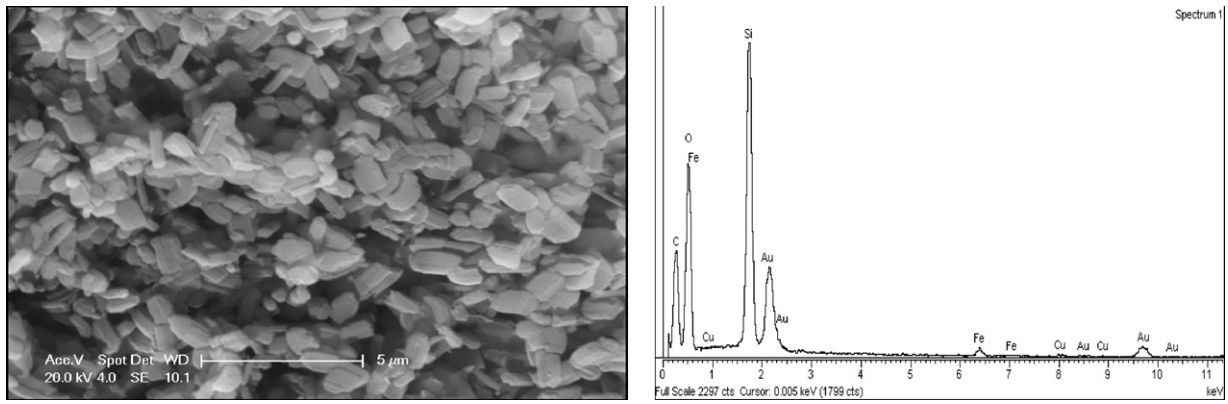
Fig. 2. SEM photo and EDX profile of Fe/SBA-15.
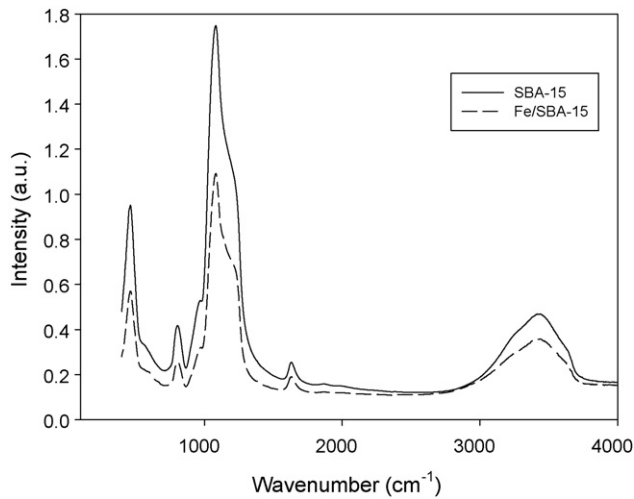

Fig. 3. FT-IR spectra of SBA-15 and Fe/SBA-15.

tions of DCP on SBA-15 and Fe/SBA-15 are 25 and 18 mg/g, respectively. Two isotherm models, Langmuir (Eq. (1)) and Freundlich isotherms (Eq. (2)), were employed to fit the experimental data.

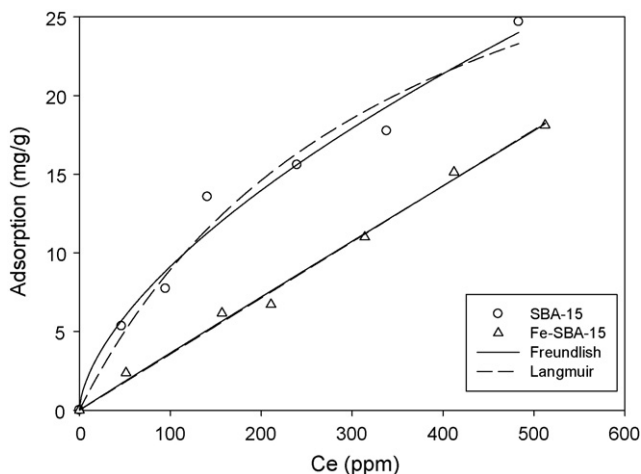$$q = \frac{q_{max}bc}{1 + bc} \qquad (1)$$

$$q = K_F c^{1/n} \qquad (2)$$

where q is the adsorption capacity (mg/g) at an equilibrium concentration and c is the equilibrium concentration (mg/L). q_{max} is monolayer adsorption and b is the Langmuir constant. K is the Freundlich constant and n is also a constant, related to adsorption capacity and intensity of adsorption, respectively.

Fig. 4 shows the fitted curves of two isotherms and the parameters obtained are given in Table 1. As seen, the two isotherms present similar curves to the experimental data, however, the Langmuir parameter for Fe/SBA-15 seems in practical.

Several investigations have been reported for 2,4-dichlorophenol adsorption on different adsorbents as listed in Table 2. As compared with activated carbons, SBA-15 and Fe/SBA-15 exhibit lower adsorption and can have a comparable adsorption with some agricultural waste derived carbons.

3.3. Kinetic study of 2,4-dichlorophenol oxidation

Fig. 5 shows the degradation of DCP at varying initial concentrations and it is seen that a complete decomposition of DCP will take about 8–10 h depending on initial DCP concentration. At low concentration of 50 ppm, DCP degradation is much faster with complete decomposition at 400 min while the degradation shows a slower rate at higher concentration. For DCP concentration of 200 ppm, degradation efficiency at 600 min is 85%.

Chaliha and Bhattacharyya [22] have conducted catalytic wet oxidation of DCP in water with Mn(II)-MCM41 and H_2O_2. The conversion of DCP on impregnated Mn(II)-MCM41 and directly synthesised Mn(II)-MCM41 with H_2O_2 was 78.0% and 55.1%,

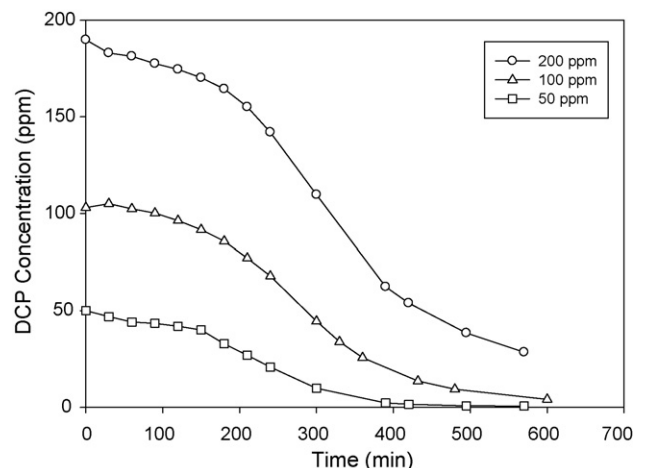**Fig. 4.** Adsorption isotherm of DCP on Fe/SBA-15.

Fig. 5. DCP degradation at various initial concentration. Catalyst loading = 0.05 g.

Table 1
Parameters of Langmuir and Freundlich isotherms for DCP adsorption on SBA-15 and Fe/SBA-15.

Material	Langmuir			Freundlich		
	q_{max} (mg/g)	b (L/mg)	R^2	K	n	R^2
SBA-15	40.2	2.85×10^{-3}	0.972	0.540	0.614	0.977
Fe/SBA-15	1.02×10^4	3.50×10^{-6}	0.994	0.0386	0.988	0.994
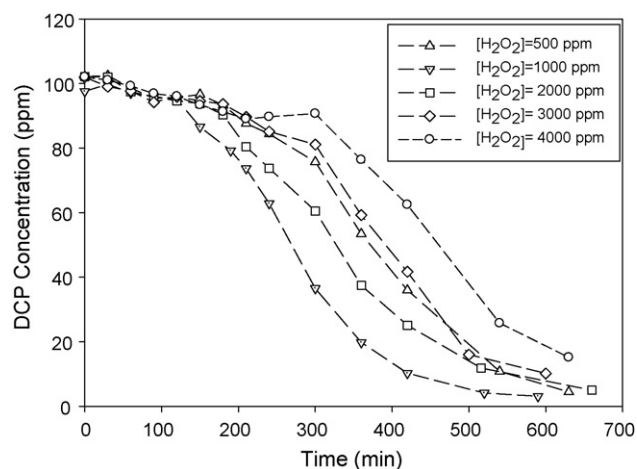
Fig. 6. Effect of H_2O_2 concentration on DCP degradation. Catalyst loading = 0.05 g.

Fig. 7. Effect of Fe loading on SBA-15 on DCP degradation.

respectively, in 5 h. They further tested Fe(III)-, Co(II)- and Ni(II)-impregnated MCM41 for wet oxidative destruction of DCP in water and found that the DCP destruction in a 1:1 molar mixture with H_2O_2 was 12.6%, 19.7% and 35.4% with Fe(III)-, Ni(II)-, and Co(II)-MCM41, respectively, in 15 min of reaction time and was 38.6%, 55.1% and 50.4% in 300 min under 0.2 MPa, 80 °C, catalyst load of 2 g/L and DCP concentration of 5×10^{-3} M. Also the DCP conversion decreased with increased DCP concentration [23]. Luo et al. [6] reported catalytic property of Fe–Al pillared clay for Fenton oxidation of phenol by H_2O_2. The heterogeneous Fenton reaction exhibited an induction period due to an activation process of the surface iron species followed by a fast oxidation of phenol. These results are similar to the observation of this investigation.

Fig. 6 shows the effect of H_2O_2 concentration on DCP degradation. The increase in H_2O_2 concentration increases the rate of degradation of DCP. However, excessive addition of H_2O_2 results in a decrease in degradation rate. From Fig. 6, it is seen that DCP degradation will achieve the maximum at H_2O_2 concentration of 1000 ppm. When H_2O_2 concentration is higher than 1000 ppm, DCP degradation rate is significantly reduced. Many investigations have presented the similar observation that higher H_2O_2 concentration will suppress the degradation rate and efficiency of organics [1]. The reduction in the reaction rate is due to the fact that excess amount of H_2O_2 acts as a scavenger to the active hydroxyl radical as per the following reaction (Eq. (3)). The radical of $HO_2^\bullet$ shows much less reaction rate than $OH^\bullet$, resulting in low DCP degradation.

$$H_2O_2 + OH^\bullet \rightarrow H_2O + HO_2^\bullet \qquad (3)$$

Table 2
A comparison of DCP adsorption on various adsorbents.

Adsorbent	Maximum monolayer adsorption capacity (mg/g)	Refs.
Oil palm empty fruit bunch carbon	232	[17]
Maize cob carbon	18	[18]
Palm pith carbon	19	[19]
Activated carbon fibre	372	[20]
KOH activated char	217–728	[21]
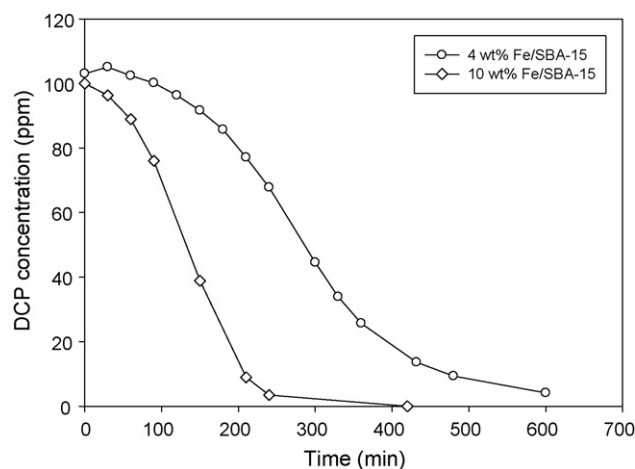
Fig. 7 displays the effect of Fe loading on SBA-15 on DCP degradation. As shown, higher loading of Fe on SBA-15 will significantly increase DCP degradation rate and efficiency. At 4 wt% Fe, a complete DCP degradation will take 10 h while at 10 wt% Fe, the degradation will take 5 h. This is due to the higher activation rate between Fe and H_2O_2 for $OH^\bullet$ generation at enhanced Fe loading on SBA-15.

Fig. 8 presents the effect of Fe/SBA-15 loading in solution on DCP degradation. Increasing amount of the catalyst has dual significance on the process of combined adsorption and oxidation. It provides additional surface area for adsorption and also additional amount of Fe for the formation of OH radicals. As seen in Fig. 8, increasing the catalyst loading in solution enhances the DCP degradation. At 0.025 g, DCP degradation is slow with the removal efficiency of 20% after 10 h, however, the degradation efficiency will reach 100% at 4 h at catalyst loading of 0.1 g.

The effect of solution pH on DCP degradation using Fe/SBA-15 and H_2O_2 was also investigated and the results are shown in Fig. 9.
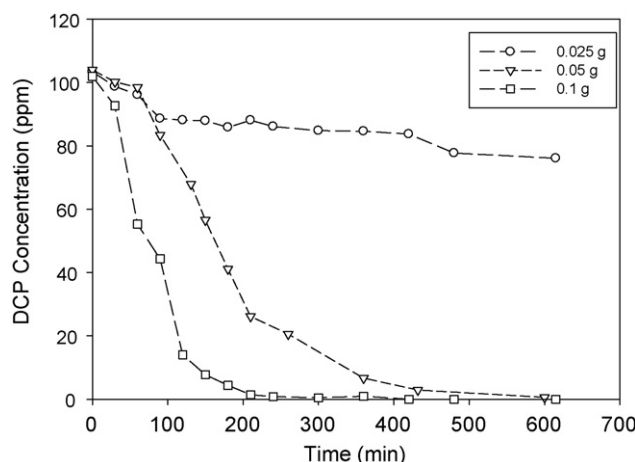

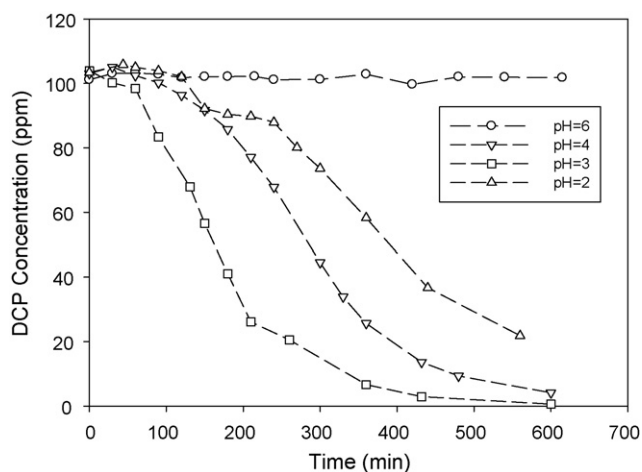**Fig. 8.** Effect of Fe/SBA-15 loading in solution on DCP degradation.

Fig. 9. Effect of solution pH on DCP degradation. Catalyst loading = 0.05 g.

Fig. 11. Performance of recycled Fe/SBA-15 in three catalytic tests.

The results indicate that pH has a significant influence on the reaction rate. It is observed that an increase in the solution acidity from pH 6 to 3 increases the reaction rate and the reaction rate reaches the maximum at pH 3. At further increased acidity of pH 2, DCP degradation rate, however, gets significantly reduced. At pH 2, DCP degradation efficiency is 80% at 500 min. While at pH 6, DCP shows no significant decomposition after 10 h, suggestion no oxidation reaction occurred. Oliveira et al. [24] investigated the oxidation of 2,4-dichlorophenol with homogeneous Fenton's reagent and have indicated the optimum pH to be around 3.5. This is similar to this investigation.

Fig. 10 presents TOC variation at different conditions in DCP degradation with Fe/SBA-15 and H_2O_2. One can see that TOC changes with Fe loading on SBA-15 and Fe/SBA-15 loading in the solution. In general, high Fe loading will get higher TOC removal. At 4 wt% of Fe on SBA-15 at 0.025 g in solution the TOC removal will be 12% at 10 h and reaches 20% at 25 h. Compared with DCP degradation efficiency at the same conditions (Fig. 8), TOC removal efficiency is lower than DCP degradation efficiency. This suggests that the intermediates produced during the decomposition of DCP would take a longer time to fully decompose and also could not be completely removed. At 10 wt% of Fe on SBA-15 at 0.05 g in solution, TOC removal can be achieved at 30% and 60% at 10 and 30 h, respectively. These are also lower compared with DCP degradation efficiency.
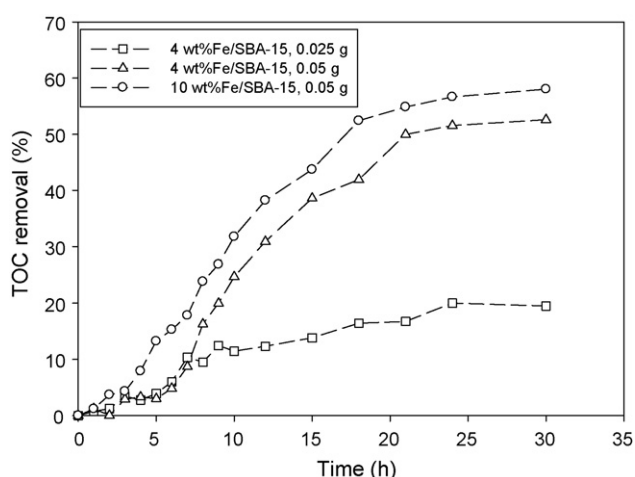
Botas et al. [15] prepared iron-containing catalysts on mesostructured SBA-15 silica and non-ordered mesoporous silica with iron loadings between 10 and 15 wt%. They tested the catalysts in phenol degradation and found that these catalysts exhibited high catalytic performances with TOC reduction of 65% and 25%, respectively. Our results are comparable to their observations.

Fig. 11 presents the performance of Fe/SBA-15 in DCP degradation after catalyst recycling with filtration and water washing. In the second run, DCP degradation profile is much similar to the first test and degradation of DCP shows a bit slow in the third run. This suggests the stable performance of Fe/SBA-15 in heterogeneous Fenton oxidation. Measurements of Fe ion in solution found undetectable metal ion present in solution, indicating much less Fe leaching from the catalyst.

Martinez et al. [12] investigated heterogeneous photo-Fenton degradation of phenolic aqueous solutions at near UV–vis irradiation using Fe/SBA-15 prepared by co-condensation and found much less Fe leaching. Sabhi and Kiwi [25] carried out the degradation of 2,4-dichlorophenol on Nafion-Fe (1.78%) in the presence of H_2O_2 under visible light irradiation. The Nafion-Fe was seen to be effective over many cycles without leaching out Fe^{3+} ions into the solution. It was found that the degradation was controlled by mass transfer at the surface of the Nation-Fe membrane. Luo et al. [6] also reported Fe leaching from Fe-Al pillared clay in Fenton oxidation of phenol by H_2O_2 with no obvious deactivation of recycled catalysts.

It has been proposed that heterogeneous Fenton oxidation occurs at the surface via Fe oxide active sites with the formation of peroxide complex species and then following a series of dissociation reactions to produce peroxide radical [12]. In this investigation, XRD and FT-IR could not identify Fe oxide. However, EDX indicated the presence of Fe species on Fe/SBA-15, which suggests the strong binding of Fe with Si framework and much small particle size of Fe in the inner pores. Thus the possible reactions involved can be proposed as follows:

$$SiO_2\text{-}Fe^{3+} + H_2O_2 \rightarrow SiO_2\text{-}Fe^{3+}\text{-}H_2O_2^\bullet \rightarrow SiO_2\text{-}Fe^{2+} + HO_2^\bullet \quad (4)$$

$$SiO_2\text{-}Fe^{2+} + H_2O_2 \rightarrow SiO_2\text{-}Fe^{3+} + 2OH^\bullet \quad (5)$$

$$DCP + HO_2^\bullet \rightarrow CO_2 + H_2O \quad (6)$$

$$DCP + OH^\bullet \rightarrow CO_2 + H_2O \quad (7)$$
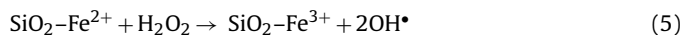
4. Conclusion

Impregnation of Fe oxide on SBA-15 will not significantly change the mesoporous structure of SBA-15 support and Fe/SBA-15 shows low adsorption of 2,4-dichlorophenol from aqueous solution.

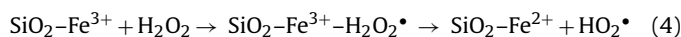**Fig. 10.** TOC removal during DCP degradation at varying catalyst loading.

However, Fe loaded SBA-15 produces promising results for heterogeneous activation of H_2O_2 for oxidation of 2,4-dichlorophenol in water. At pH 3, complete destruction of DCP can be obtained within 7–8 h. Addition of 0.1 g of catalyst results in complete degradation of DCP within 3 h. TOC analysis shows approximately 60 percent mineralisation of DCP. Fe/SBA-15 also exhibits stable activity in several cycles with less Fe leaching.

References

[1] S. Wang, A comparative study of Fenton and Fenton-like reaction kinetics in decolourisation of wastewater, Dyes and Pigments 76 (2008) 714–720.

[2] T.L.P. Dantas, V.P. Mendonça, H.J. José, A.E. Rodrigues, R.F.P.M. Moreira, Treatment of textile wastewater by heterogeneous Fenton process using a new composite Fe_2O_3/carbon, Chemical Engineering Journal 118 (2006) 77–82.

[3] R.C.C. Costa, F.C.C. Moura, J.D. Ardisson, J.D. Fabris, R.M. Lago, Highly active heterogeneous Fenton-like systems based on Fe^0/Fe_3O_4 composites prepared by controlled reduction of iron oxides, Applied Catalysis B: Environmental 83 (2008) 131–139.

[4] J. Deng, J. Jiang, Y. Zhang, X. Lin, C. Du, Y. Xiong, $FeVO_4$ as a highly active heterogeneous Fenton-like catalyst towards the degradation of Orange II, Applied Catalysis B: Environmental 84 (2008) 468–473.

[5] S. Yang, H. He, D. Wu, D. Chen, X. Liang, Z. Qin, M. Fan, J. Zhu, P. Yuan, Decolorization of methylene blue by heterogeneous Fenton reaction using $Fe_{3-x}Ti_xO_4$ ($0 \leq x \leq 0.78$) at neutral pH values, Applied Catalysis B: Environmental 89 (2009) 527–535.

[6] M. Luo, D. Bowden, P. Brimblecombe, Catalytic property of Fe–Al pillared clay for Fenton oxidation of phenol by H_2O_2, Applied Catalysis B: Environmental 85 (2009) 201–206.

[7] E.G. Garrido-Ramírez, B.K.G. Theng, M.L. Mora, Clays and oxide minerals as catalysts and nanocatalysts in Fenton-like reactions—a review, Applied Clay Science 47 (2010) 182–192.

[8] Q. Liao, J. Sun, L. Gao, Degradation of phenol by heterogeneous Fenton reaction using multi-walled carbon nanotube supported Fe_2O_3 catalysts, Colloids and Surfaces A: Physicochemical and Engineering Aspects 345 (2009) 95–100.

[9] S. Wang, Ordered mesoporous materials for drug delivery, Microporous and Mesoporous Materials 117 (2009) 1–9.

[10] S. Wang, H. Li, Structure directed reversible adsorption of organic dye on mesoporous silica in aqueous solution, Microporous and Mesoporous Materials 97 (2006) 21–26.

[11] N. Gokulakrishnan, A. Pandurangan, P.K. Sinha, Removal of citric acid from aqueous solution by catalytic wet peroxidation using effective mesoporous Fe-MCM-41 molecular sieves, Journal of Chemical Technology and Biotechnology 82 (2007) 25–32.

[12] F. Martinez, G. Calleja, J.A. Melero, R. Molina, Heterogeneous photo-Fenton degradation of phenolic aqueous solutions over iron-containing SBA-15 catalyst, Applied Catalysis B: Environmental 60 (2005) 181–190.

[13] J.A. Melero, G. Calleja, F. Martinez, R. Molina, Nanocomposite of crystalline Fe_2O_3 and CuO particles and mesostructured SBA-15 silica as an active catalyst for wet peroxide oxidation processes, Catalysis Communications 7 (2006) 478–483.

[14] H. Lim, J. Lee, S. Jin, J. Kim, J. Yoon, T. Hyeon, Highly active heterogeneous Fenton catalyst using iron oxide nanoparticles immobilized in alumina coated mesoporous silica, Chemical Communications (2006) 463–465.

[15] J.A. Botas, J.A. Melero, F. Martinez, M.I. Pariente, Assessment of Fe_2O_3/SiO_2 catalysts for the continuous treatment of phenol aqueous solutions in a fixed bed reactor, Catalysis Today 149 (2010) 334–340.

[16] D.Y. Zhao, J.L. Feng, Q.S. Huo, N. Melosh, G.H. Fredrickson, B.F. Chmelka, G.D. Stucky, Triblock copolymer syntheses of mesoporous silica with periodic 50 to 300 angstrom pores, Science 279 (1998) 548–552.

[17] F.W. Shaarani, B.H. Hameed, Batch adsorption of 2,4-dichlorophenol onto activated carbon derived from agricultural waste, Desalination 255 (2010) 159–164.

[18] M. Sathishkumar, A.R. Binupriya, D. Kavitha, R. Selvakumar, R. Jayabalan, J.G. Choi, S.E. Yun, Adsorption potential of maize cob carbon for 2,4-dichlorophenol removal from aqueous solutions: equilibrium, kinetics and thermodynamics modeling, Chemical Engineering Journal 147 (2009) 265–271.

[19] M. Sathishkumar, A.R. Binupriya, D. Kavitha, S.E. Yun, Kinetic and isothermal studies on liquid-phase adsorption of 2,4-dichlorophenol by palm pith carbon, Bioresource Technology 98 (2007) 866–873.

[20] J.-P. Wang, H.-M. Feng, H.-Q. Yu, Analysis of adsorption characteristics of 2,4-dichlorophenol from aqueous solutions by activated carbon fiber, Journal of Hazardous Materials 144 (2007) 200–207.

[21] F.-C. Wu, R.-L. Tseng, C.-C. Hu, Comparisons of pore properties and adsorption performance of KOH-activated and steam-activated carbons, Microporous and Mesoporous Materials 80 (2005) 95–106.

[22] S. Chaliha, K.G. Bhattacharyya, Catalytic wet oxidation of 2-chlorophenol, 2,4-dichlorophenol and 2,4,6-trichlorophenol in water with Mn(II)-MCM41, Chemical Engineering Journal 139 (2008) 575–588.

[23] S. Chaliha, K.G. Bhattacharyya, Fe(III)-, Co(II)- and Ni(II)-impregnated MCM41 for wet oxidative destruction of 2,4-dichlorophenol in water, Catalysis Today 141 (2009) 225–233.

[24] R. Oliveira, M.F. Almeida, L. Santos, L.M. Madeira, Experimental design of 2,4-dichlorophenol oxidation by Fenton's reaction, Industrial & Engineering Chemistry Research 45 (2006) 1266–1276.

[25] S. Sabhi, J. Kiwi, Degradation of 2,4-dichlorophenol by immobilized iron catalysts, Water Research 35 (2001) 1994–2002.